

Evidence for Penning Ionization in the Generation of Electronically Excited States of Transition Metal Cations by Laser Vaporization

Yehia M. Ibrahim, Edreese H. Alsharaeh, and M. Samy El-Shall*

Department of Chemistry, Virginia Commonwealth University, Richmond, Virginia 23284-2006

Received: January 27, 2004

We report the first evidence for the involvement of Penning ionization in the production of electronically excited state transition metal ions by laser vaporization in the presence of argon carrier gas. The use of argon as a carrier gas has been usually considered to be a more efficient cooling and quenching gas of the excited-state species. The current results show that this view is no longer valid and under certain conditions, where metastable argon atoms can be generated through the laser plasma vaporization, efficient production of electronic excited states of transition metal ions can result. The effect of Penning ionization is demonstrated for the production of excited states of Ni^+ , Nb^+ , and Pt^+ ions through the coupling of the laser vaporization/ionization of metals and the mass-selected ion mobility techniques. The current finding has significant implications not only for understanding the mechanisms of ion production by laser-surface interactions, but also for developing new approaches to study state selected ion–molecule reactions.

Over the past two decades, pulsed laser vaporization/ionization (LVI) has been established as a powerful tool to generate a variety of gas-phase metal ions, clusters, and nanoparticles for a wide range of studies including ion–molecule reactions, ion thermochemistry, solvation dynamics, and spectroscopy of cluster ions.^{1–5} Laser vaporization of metals using nanosecond lasers typically generates a large number of metal atoms ($\approx 10^{14}$), a small fraction of singly charged atomic ions ($\approx 10^6$), and a much smaller fraction of multiply charged ions.^{1–4} Other species that are normally generated include fast electrons accelerated by the absorption of laser radiation. Generation of the metal ions is viewed as a combination of thermal, plasma, and multiphoton ionizations. In addition, electron impact (EI) via collisions of fast electrons with metal atoms is considered to play a major role in the ion production, particularly under confined plasma conditions.^{1–3} Although the presence of excited-state ions in LVI has been supported by the observation of endothermic reactions, direct identification of the excited states produced by LVI has not been reported.^{3,4} On the other hand, a few studies have reported the characterization of the electronic states of transition metal ions produced by EI and glow discharge (GD).^{6–8} These studies became possible with the application of the ion mobility technique to separate the electronic states of metal ions since ground and excited-state ions exhibit different collision cross sections with a helium buffer gas placed inside a drift tube (also known as electronic state ion chromatography, IC).^{6–10}

The application of IC to metal ions produced by LVI can provide critical information on the nature of the electronic states accessible within different LVI experiments (for example, by using IR, visible, or UV lasers under different power density regimes) and on the relative populations of different states as compared to the ions generated by EI and GD methods. Furthermore, it would be possible to reveal the different mechanisms by which excited metal ion states might be produced in the LVI experiments. Here, we report, for the first time, the application of IC to characterize the electronic states of atomic metal ions generated by LVI, and provide evidence

for the involvement of Penning ionization in the production of excited state ions. These results have significant implications not only for understanding the mechanisms of ion production by laser-surface interactions but also for developing new approaches to study state selected ion–molecule reactions.

Our mass-selected ion drift cell apparatus has been described previously.^{11,12} The metal ions were generated by pulsed LVI using the second harmonics of a Nd:YAG laser (532 nm, 20–60 mJ/pulse operated at 30 Hz). The metal ions were entrained in a beam of a carrier gas (He, Ar, Ne, or N_2) generated by a supersonic expansion through a conical nozzle (200 μm diameter) in pulses of 200–300 μs duration at repetition rates of 30 Hz. Figure 1 displays a schematic of the LVI setup coupled to the ion mobility system. The mass-selected metal ions are injected as a narrow pulse of ions (1 to 10 μs) into a drift cell containing 2 Torr of helium at room temperature. Upon exiting the cell, the ions are collected and refocused to a second quadrupole for analysis and detection. The arrival time distributions (ATDs) are measured as a function of P/V where P is the helium pressure, and V is the voltage across the drift cell.

We examined the electronic states of the laser-generated Ti^+ , V^+ , Cr^+ , Mn^+ , Fe^+ , Co^+ , Ni^+ , Cu^+ , Zn^+ , Zr^+ , Nb^+ , Pd^+ , Ag^+ , Cd^+ , Pt^+ , and Au^+ ions. For the purpose of this letter, we focus on Ni^+ , Pt^+ , Nb^+ , and Ag^+ as elaborated below. The results are summarized in Table 1.

Figures 2a and 2b display the ATDs of Ni^+ produced in He and Ar expansions, respectively. In both cases, the spectrum contains two well-resolved peaks assigned to the excited ($4s\ 3d^8$, high mobility) and ground ($3d^9$, low mobility) states of Ni^+ . The reduced mobilities for the excited and ground states were measured as 24.1 and 16.2 $\text{cm}^2\ \text{V}^{-1}\ \text{s}^{-1}$, respectively, in excellent agreement with the literature values as shown in Table 1. However, we note that the excited-state populations of the transition metal ions obtained by LVI are significantly lower than the populations measured for ions generated by EI of organometallic compounds.⁶ For example, the fraction of the ground-state population measured at 17 eV ionizing energy (the

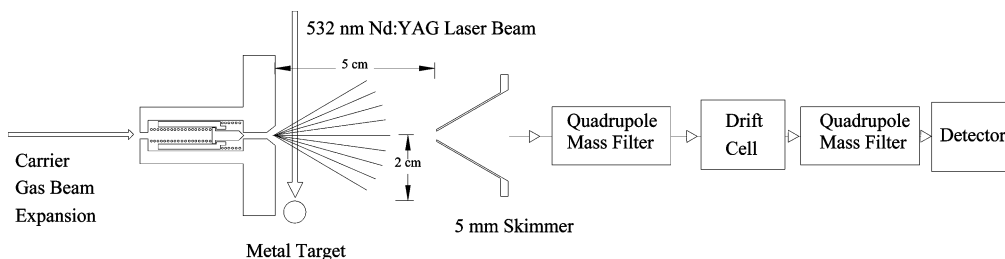


Figure 1. LVI setup coupled to the mass-selected ion mobility system (see ref 11 for details).

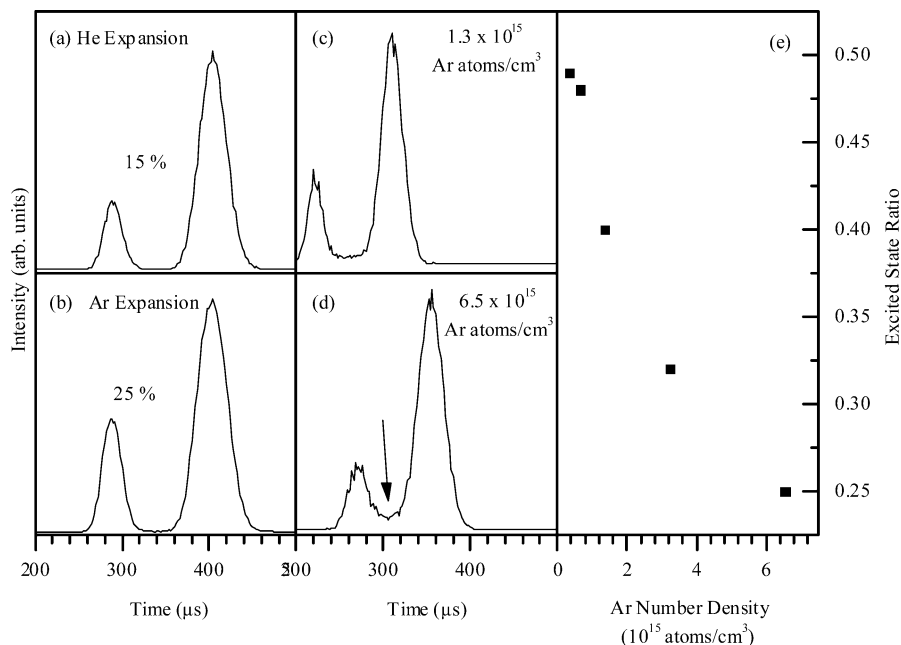


Figure 2. ATDs (in pure helium) of Ni^+ produced by LVI in (a) helium and (b) argon expansions. (c,d) ATDs of Ni^+ in the drift cell containing different concentrations of Ar in He. (e) Excited-state population of Ni^+ as a function of the Ar concentration in the drift cell.

TABLE 1: Measured Reduced Mobilities (K_0) and State Populations (Pop %) of Selected TM Ions

ion	state	conf	energy (eV) ^a	pop. %	K_0		
					<i>b</i>	<i>c</i>	<i>d</i>
Ni^+	^2D	3d^9	0.075	64–87	16.2	16.3	16.2
	^4F	$3\text{d}^84\text{s}$	1.160				
	^2F	$3\text{d}^84\text{s}$	1.757				
	^4P	$3\text{d}^84\text{s}$	2.899				
Pt^+	^2D	5d^9	0.418	80–50	18.3	20.2	20.2
	^4F	$5\text{d}^86\text{s}$	1.177				
	^4P	$5\text{d}^86\text{s}$	2.366				
	^2F	$5\text{d}^86\text{s}$	2.529				
Nb^+	^5D	4d^4	0.096	74–55	15.5	19.7	18
	^3P	4d^4	0.833				
	^3H	4d^4	1.225				
	^5F	$4\text{d}^35\text{s}$	0.421				
Ag^+	^3F	$4\text{d}^35\text{s}$	0.990	78–66	17.7	22.1	18
	^1S	4d^{10}	0.000				
	^2D	$4\text{d}^95\text{s}$	5.034				

^a Reference 13, average over *J* levels. ^b This work. ^c Reference 6. ^d Reference 10.

AP of Ni^+ from $\text{Ni}(\text{CO})_4 = 14.75$ eV) is only 60%,⁶ while in our experiments with a low laser power of 1.5×10^{10} W/cm² at least 87% ground-state Ni^+ can be produced. We also note that the populations of the excited states do not increase sharply with the laser power in the LVI experiments using the second harmonic of the YAG laser. This may result from entraining the laser-generated ions in the cold Ar beam, which deactivates a significant portion of the excited ions before entering the drift tube.

The assignments of electronic states given in Table 1 are supported by collisional deactivation studies using different concentrations of Ar inside the drift cell. It is clear, from the data shown in Figures 2c and 2d, that the collisions of excited-state Ni^+ with Ar atoms efficiently quench the excitation energy and thus result in increasing the population of the ground state ions. The conversion of states with different configurations in the drift cell usually appears as filling between the two mobility peaks corresponding to the two states as observed in Figure 2d. The population of the excited states is measured as the ratio of the area of the ATD peak assigned to the excited state to the sum of the areas of the excited- and ground-state ATD peaks. This population exhibits a sharp decrease with the Ar number density inside the drift cell as shown in Figure 2e. From these data, the deactivation rate coefficient is estimated as 5×10^{-14} cm³ s⁻¹. This is consistent with the expected greater collisional relaxation efficiency of Ar over He. Similar trends have been observed with other transition metal ions. However, the data shown in Figures 2a and 2b indicate that the relative amount of excited-state Ni^+ increases more in Ar than in He expansions. This could suggest the presence of an additional mechanism that favors the production of excited-state Ni^+ in the presence of Ar. A simple mechanism could be charge transfer from Ar^+ assuming that the current LVI experiment can produce energetic species with more than 15.5 eV (the ionization potential of Ar).¹³ However, Ar^+ ions were never observed under the current experimental conditions. Another possible mechanism could be Penning ionization via Ar metastable atoms, which are known to occur at 11.5 and 11.7 eV.^{13,14} These metastables could be

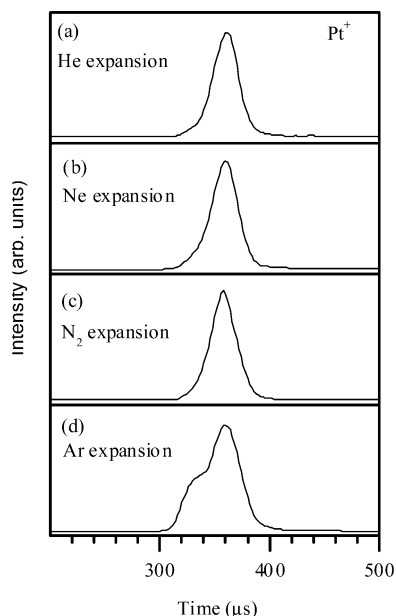


Figure 3. ATDs (in pure helium) of Pt^+ produced by LVI in (a) helium, (b) neon, (c) nitrogen, and (d) argon expansions.

produced in the laser plume and also via collisions of Ar atoms with the *fast* electrons produced by the laser plasma vaporization. The collisions of metastable Ar^* with the Ni atoms produced by laser vaporization would then generate the excited-state Ni^+ since the ionization potential of Ni ($\text{IP} = 7.60 \text{ eV}$) plus the excitation energy [$E(^4\text{P}) - E(^2\text{D}) = 2.899 - 0.075 = 2.82 \text{ eV}$] is $10.4 \text{ eV} < 11.5 \text{ eV}$.¹³

To further test the possibility of Penning ionization, we measured the ATDs of Pt^+ produced by LVI in He, Ne, N_2 , and Ar expansions as shown in Figures 3 (a–d, respectively). The ATDs of the ions produced in He, Ne, and N_2 are very similar and appear to contain small contributions from high mobility configurations as evident by the unresolved tailing at the early time of the mobility peak. This high mobility configuration is clearly enhanced in the presence of Ar as compared to He, Ne, or N_2 . The high mobility component is assigned to excited-state Pt^+ , which appears to be efficiently produced in the presence of Ar during LVI. Experiments showed that the population of the excited Pt^+ decreased when the distance between the metal target and the nozzle orifice producing the Ar expansion was increased (see Figure 1), thus supporting the generation of metastable Ar^* . As in the case of Ni^+ , the production of excited-state Pt^+ via collisions of Ar^* with Pt atoms is energetically possible since $\text{IP}(\text{Pt}) + [E(^2\text{F}) - E(^2\text{D})] = 11.1 \text{ eV} < 11.5 \text{ eV}$.¹³ It should be noted that the metastable Ar^* atoms are favorably produced as compared to other carrier gas atoms such as He due to the higher probability of producing Ar^* (11.5 eV) vs He^* (19.7 eV),¹⁴ and also due to the significantly higher cross section for Penning ionization by Ar^* .¹⁴

Another example where the energetics allow the generation of excited-state ions by Penning ionization from Ar^* is Nb^+ , since $\text{IP}(\text{Nb}) + [E(^3\text{F}) - E(^5\text{D})] = 8.65 \text{ eV}$. Figures 4a and 4b compare the ATDs of Nb^+ generated by LVI in He and Ar expansions. Again, the population of excited states is significantly enhanced in the presence of Ar during the LVI. The difference in the excited-state populations produced in He and Ar could serve as a measure of the lower limit of the fraction of ions produced by Penning ionization (about 20% under the experimental conditions of Figures 4a and 4b). For comparison, the relative population of excited-state Ag^+ produced by LVI

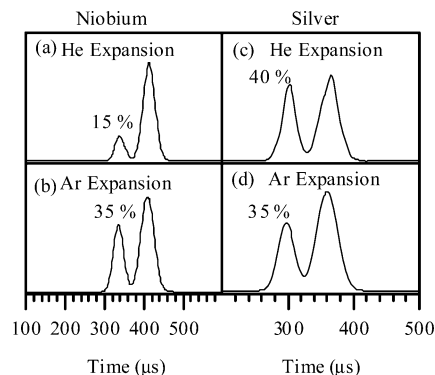


Figure 4. ATDs (in pure helium) of Nb^+ and Ag^+ produced by LVI in He and Ar expansions.

in the presence of Ar is actually less than that produced in He expansion, as shown in the ATDs displayed in Figures 4c and 4d. This is consistent with the absence of a Penning ionization mechanism in this system since $\text{IP}(\text{Ag}) + [E(^2\text{D}) - E(^1\text{S})] = 12.6 \text{ eV} > 11.5 \text{ eV}$. In this case, the excited states of Ag^+ are produced by the other LVI mechanisms such as EI by *fast* electrons and thermal desorption, and therefore the net effect of collision with Ar was relaxation of these Ag^{+*} excited states.

In summary, we report the first evidence for the involvement of Penning ionization in the production of excited-state ions by laser vaporization in the presence of argon carrier gas. The use of argon as a carrier gas has been usually considered to be a more efficient cooling and quenching gas of the excited-state species. The current results show that this view is no longer valid and under certain conditions, where metastable argon atoms can be generated through the laser plasma vaporization, efficient production of electronic excited states of transition metal ions can result. The current finding has significant implications not only for understanding the mechanisms of ion production by laser-surface interactions but also for developing new approaches to study state selected ion–molecule reactions. For example, it is interesting to see if LVI experiments using different lasers (UV or IR radiation) can access higher excitation energies or result in different populations of excited states as compared to the current LVI experiments using the second harmonic of the YAG laser. These experiments (currently underway in our laboratory) will provide unavailable information on the energy distribution of the *fast* electrons produced in different LVI experiments.

Acknowledgment. We thank the National Science Foundation for support of this research (CHE-9816536).

References and Notes

- (1) Anisimov, S. I.; Luk'yanchuk, B. S. *Physics-Uspekhi* **2002**, *45*, 293–324.
- (2) Dreyfus, R. W. *Laser Ablation of Electronic Materials: Basic Mechanisms and Applications*; Fogarassy, E., Ed.; Elsevier Publishers: London, 1992.
- (3) *Laser Ablation: Mechanisms and Applications* (Lecture Notes in Physics); Miller, J. C.; Haglund, R. F., Jr., Eds.; Springer-Verlag: Berlin, 1991; Vol. 389.
- (4) Kang, H.; Beauchamp, J. L. *J. Phys. Chem.* **1985**, *89*, 3364–3367.
- (5) Blomberg, M.; Yi, S. S.; Noll, R. J.; Weisshaar, J. C. *J. Phys. Chem. A* **1999**, *103*, 7254–7267.
- (6) Kemper, P. R.; Bowers, M. T. *J. Phys. Chem.* **1991**, *95*, 5134–5146.

- (7) Twiddy, N. D.; Mohebati, A.; Tichy, M. *Int. J. Mass Spectrom. Ion Processes* **1986**, *74*, 251.
- (8) Hansel, A.; Richter, R.; Herman, Z.; Lindinger, W. *J. Chem. Phys.* **1991**, *94*, 8632–8633.
- (9) Bowers, M. T.; Kemper, P. R.; von Helden, G.; van Koppen, P. A. *M. Science* **1993**, *260*, 1446–1451. Clemmer, D. E.; Hunter, J. M.; Shelimov, K. B.; Jarrold, M. F. *Nature* **1994**, *372*, 248–250.
- (10) Taylor, W. S.; Campbell, A. C.; Barnas, D. F.; Babcock, L. M.; Linder, C. B. *J. Phys. Chem. A* **1997**, *101*, 2654–2661. Taylor, W. S.; Spicer, E. M.; Barnas, D. F. *J. Phys. Chem. A* **1999**, *103*, 643–650.
- (11) Rusyniak, M. J.; Ibrahim, Y. M.; Wright, D.; Khanna, S. N.; El-Shall, M. S. *J. Am. Chem. Soc.* **2003**, *125*, 12001–12013.
- (12) Rusyniak, M.; Ibrahim, Y.; Alsharaeh, E.; Meot-Ner, M.; El-Shall, M. S. *J. Phys. Chem. A* **2003**, *107*, 7656–7666.
- (13) Moore, C. E. *Atomic Energy Levels*, Natl. Stand. Ref. Data Ser., Natl. Bur. Stand. (NSRDS–NBS); 1971, 35. Linstrom, P. J., Mallard, W. G., Eds., NIST Chemistry WebBook; NIST Standard Reference Database Number 69, March 2003; National Institute of Standards and Technology: Gaithersburg, MD, 20899 (<http://webbook.nist.gov>).
- (14) Siska, P. E. *Rev. Mod. Phys.* **1993**, *65*, 337–412.